



A promising composite solid electrolyte incorporating LLZO into PEO/PVDF matrix for all-solid-state lithium-ion batteries

Jun Li^{1,2} · Kongjun Zhu¹ · Zhongran Yao¹ · Guoming Qian¹ · Jie Zhang^{1,2} · Kang Yan¹ · Jing Wang¹

Received: 7 June 2019 / Revised: 15 September 2019 / Accepted: 23 October 2019 / Published online: 10 November 2019
© Springer-Verlag GmbH Germany, part of Springer Nature 2019

Abstract

Solid electrolytes should be sought to exhibit high conductivity, good thermostability, and excellent mechanical properties for realizing excellent performance of lithium-ion batteries. In this study, we optimize the composition of poly(ethylene oxide)/poly(vinylidene fluoride) (PEO/PVDF) matrix and introduce $\text{Li}_{6.2}\text{Ga}_{0.1}\text{La}_3\text{Zr}_{1.5}\text{Bi}_{0.5}\text{O}_{12}$ (LLZO) ceramic powders into the matrix to form novel composite solid electrolytes. The PEO/PVDF blend matrix shows a low melting point and crystallinity and a high thermostability when the weight ratio of PEO and PVDF is 7:3. The electrolyte consisting of this PEO/PVDF blend matrix and 10 wt% LLZO shows the maximum conductivity ($4.2 \times 10^{-5} \text{ S cm}^{-1}$ at 30 °C). In addition, all-solid-state $\text{LiFePO}_4\|\text{Li}$ battery assembled with this solid electrolyte shows good cycling stability, which retained 96.5% of the maximum capacity after 100 cycles, and coulombic efficiency (close to 100%) at 60 °C. The $\text{Li}\|\text{Li}$ symmetric battery assembled with the solid electrolyte can be steadily cycled for more than 300 h at a current density of 0.2 mA cm^{-2} at 60 °C. Hence, the new as-synthesized solid electrolyte should be a promising electrolyte for high performance of all-solid-state batteries.

Keywords Composite solid electrolyte · Poly(ethylene oxide) · Poly(vinylidene fluoride) · LLZO · All-solid-state lithium-ion battery

Introduction

The capability of solid polymer electrolytes (SPEs) has attracted considerable attention because they can solve the safety problems in commercial lithium-ion batteries (LIBs) that use organic liquid electrolytes (e.g., leakage of organic solvents, lithium dendrite formation, internal short circuits, and flammability) [1–3]. SPEs should be sought to exhibit high conductivity, good thermal and electrochemical stabilities, and excellent mechanical properties to prepare all-solid-state LIBs with good performance [4–7].

Poly(ethylene oxide) (PEO) has been extensively studied as a polymer matrix for SPEs due to its good electrochemical

stability and excellent capability of dissolving a wide variety of lithium salts. However, PEO-based SPEs suffer from low ionic conductivity (10^{-7} to $10^{-6} \text{ S cm}^{-1}$ at 25 °C) due to high crystallinity, which slows ionic mobility. In addition, their low mechanical strength and poor thermostability may restrict their applications in LIBs [8–11].

Blending of different polymers is a simple and effective solution for controlling the physical properties within the mix compositional region. It also shows superior properties than individual components of the blend [12]. Tao et al. reported that the blend of thermoplastic polyurethane and PEO could achieve a higher ionic conductivity and better mechanical strength than the single PEO-based SPE [13]. Fan et al. prepared PEO and poly(vinylidene fluoride) (PVDF) blend based SPEs to achieve a combination of higher ionic conductivity and other better properties [14].

Adding ceramic solid electrolyte into SPE to prepare composite solid electrolyte (CSE) is another effective solution for improvement in ionic conductivity, mechanical strength, and thermostability [15]. The PEO/ LiClO_4 solid electrolyte incorporating $\text{Li}_{1.5}\text{Al}_{0.5}\text{Ge}_{1.5}(\text{PO}_4)_3$ ceramic studied by Jung et al. achieved high ionic conductivity of $2.6 \times 10^{-4} \text{ S cm}^{-1}$ at 55 °C and good stability against lithium metal [16]. Zhao et al.

✉ Kongjun Zhu
kjzhu@nuaa.edu.cn

¹ State Key Laboratory of Mechanics and Control of Mechanical Structures, Nanjing University of Aeronautics and Astronautics, Nanjing 210016, China

² College of Materials Science and Technology, Nanjing University of Aeronautics and Astronautics, Nanjing 210016, China

studied the ionic conductivity of a CSE fabricated by incorporating $\text{Li}_{10}\text{GeP}_2\text{S}_{12}$ into PEO/LiTFSI. The electrolyte showed ionic conductivity of $1.18 \times 10^{-5} \text{ S cm}^{-1}$ at 25 °C. Recently, the cubic garnet-type inorganic solid electrolyte $\text{Li}_7\text{La}_3\text{Zr}_2\text{O}_{12}$ (LLZO) has attracted considerable attention because of its chemical stability to lithium metal, high electrochemical window ($> 5 \text{ V vs. Li/Li}^+$), and high ionic conductivity ($> 10^{-4} \text{ S cm}^{-1}$ at 25 °C) [17–20]. Chen et al. studied PEO/LLZO composite electrolyte membrane, which exhibited $5.5 \times 10^{-4} \text{ S cm}^{-1}$ at 60 °C. Furthermore, the all-solid-state $\text{Li}||\text{LiFePO}_4$ cell with this membrane shows a high initial discharge capacity and good cycling and rate performance [21]. Nevertheless, the achieved ionic conductivity and mechanical properties still cannot meet the requirements of all-solid-state LIBs.

In this study, a series of composite solid electrolytes consisting of PEO, PVDF, LiTFSI, and LLZO were prepared by blending technique combined with adding ceramic solid electrolytes. PVDF was used to reduce PEO crystallinity, which is beneficial for improving ionic conductivity. In addition, it was used to improve the mechanical properties and thermostability. Furthermore, adding LLZO further improves ionic conductivity and stability against lithium metal. The CSE exhibited high conductivity, good thermostability, and excellent mechanical properties. The all-solid-state LIB with this solid electrolyte membrane, a lithium metal anode, and a LiFePO_4 cathode displayed excellent initial discharge capacity, good cyclic performance, and good stability against lithium metal.

Experimental

Starting materials

The PEO with an average relative molecular mass M_m of ~ 300000 , acetonitrile (ACN), LiNO_3 , $\text{La}(\text{NO}_3)_3 \cdot 6\text{H}_2\text{O}$, $\text{ZrO}(\text{NO}_3)_2 \cdot x\text{H}_2\text{O}$, $\text{Ga}(\text{NO}_3)_3 \cdot x\text{H}_2\text{O}$, $\text{Bi}(\text{NO}_3)_5 \cdot 5\text{H}_2\text{O}$, $\text{C}_6\text{H}_8\text{O}_7 \cdot \text{H}_2\text{O}$, $\text{C}_2\text{H}_6\text{O}_2$, and LiTFSI were acquired from Macklin. PVDF was purchased from Arkma Fluorochemical Co., Ltd. All the purchased chemical reagents were of analytical grade and used directly without any purification.

Synthesis of inorganic electrolyte LLZO powders

LLZO was synthesized via the sol–gel method. Preparing two different solutions was necessary for synthesis. In the first solution, 0.0682 mol of LiNO_3 , 0.03 mol of $\text{La}(\text{NO}_3)_3 \cdot 6\text{H}_2\text{O}$, 0.015 mol of $\text{ZrO}(\text{NO}_3)_2 \cdot x\text{H}_2\text{O}$, 0.001 mol of $\text{Ga}(\text{NO}_3)_3 \cdot x\text{H}_2\text{O}$, and 0.226 mol of $\text{C}_6\text{H}_8\text{O}_7 \cdot \text{H}_2\text{O}$ were dissolved in 100 mL of deionized water under stirring. $\text{NH}_3 \cdot \text{H}_2\text{O}$ was then added to the preceding solution until a pH value of 7 was achieved. In the second solution, 0.005 mol of

$\text{Bi}(\text{NO}_3)_5 \cdot 5\text{H}_2\text{O}$ and 0.226 mol of $\text{C}_2\text{H}_6\text{O}_2$ were mixed together. The two solutions were blended and then stirred to obtain a homogeneous solution at room temperature. Subsequently, the homogeneous solution was vaporized at 100 °C for 12 h and then dried at 250 °C for 3 h to become black gel. Finally, the obtained product was ground and calcined at 800 °C for 12 h in air atmosphere.

Preparation of composite solid electrolyte membranes

The composite solid electrolyte membranes were prepared using solution cast technique. The PEO/PVDF/LiTFSI weight ratio was fixed at 7:3:2, and the weight percentage of LLZO was varied from 5 to 15 wt% on the basis of the total PEO+PVDF+LiTFSI+LLZO weight of the CSEs. The preceding raw materials were dissolved in ACN and stirred until a highly viscous slurry was formed. Thereafter, the slurry was cast using a Teflon container and completely vacuum dried at 60 °C to form an approximately 120- μm uniform membrane. Finally, the membrane was stored in an argon-filled glove box. The composite solid electrolyte membrane synthesis process and lithium-ion conducting pathway are displayed in Fig. 1.

Characterization

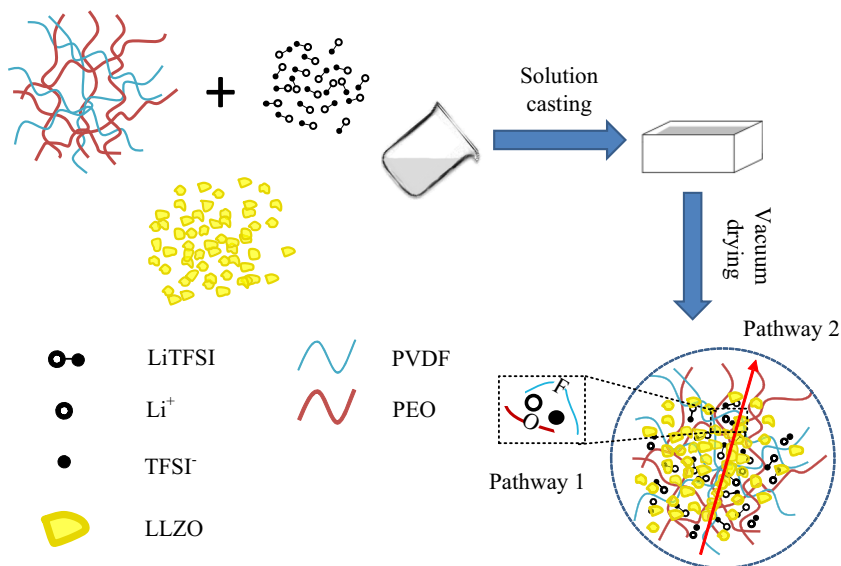
The crystal structures of LLZO powders and CSEs were analyzed using X-ray diffraction measurements (Bruker D8 Advance, Germany) of $2\theta = 10\text{--}80^\circ$ using Cu K α radiation. The morphologies of LLZO powders and CSEs were examined using an S-4800 field-emission scanning electron microscope (Hitachi, Japan). The crystallinity and melting point change of membranes were recorded using differential scanning calorimetry (DSC), and the thermal degradation of PEO and PEO/PVDF blend films was measured using thermo gravimetric analysis (TGA). The mechanical strength was tested by an Instron-3343 universal testing machine (USA) at a stretching speed of 0.667 mm s^{-1} .

A CHI660E electrochemical workstation (Shanghai Chenhua Instrument Co., Ltd.) was used to study the ionic conductivity of LLZO and CSEs over the frequency range of 0.1–1000 kHz. The solid electrolytes were presented between the two symmetrical blocking electrodes. The ionic conductivity σ (S cm^{-1}) of the electrolyte can be calculated as follows:

$$\sigma = L / (R \times S) \quad (1)$$

where L (cm), R (Ω), S (cm^2) represent the thickness of the electrolyte, the value of the resistance, and the area of the electrode, respectively.

Fig. 1 Schematic presentation of synthesis of composite solid electrolyte



The $\text{LiFePO}_4|\text{CSE}|\text{Li}$ cell was assembled to test the charge–discharge cycles using the LAND CT2001A instrument. The LiFePO_4 cathode was composed of 80 wt% LiFePO_4 , 10 wt% black acetylene, and 10 wt% PVDF. The lithium periodic stripping/plating test was conducted by a $\text{Li}|\text{CSE}|\text{Li}$ cell.

Results and discussion

The XRD patterns of the PEO/PVDF blends at various compositions are shown in Fig. 2a. All the blend membranes exhibit PEO diffraction peaks. The absence of PVDF diffraction peak can be detected with the content of PEO of more than 7:3, which suggests the homogeneous characteristic of the PEO/PVDF blend membranes. However, additional peaks around $2\theta = 20^\circ$ identified as PVDF crystalline peaks can be

observed [22], when the mass ratio of PEO and PVDF is less than 7:3. The melting and crystallization behavior was investigated using the DSC method to confirm the influence of PVDF on the crystallinity of PEO/PVDF blend membranes (Fig. 2b). All blend membranes show a defined endothermic peak between 65 and 80 °C, which is assigned to the melting point T_m of PEO. As the PVDF content increases, the endothermic peak shifts to lower temperatures. The addition of PVDF in the PEO/PVDF blend matrix can also affect the heat enthalpy ΔH_m and the crystallinities χ_c . The preceding data are summarized in Table 1. The crystallinities of the blended membrane are calculated as follows:

$$\chi_c = \Delta H_m / (\Delta H_{\text{PEO}} f_{\text{PEO}}) \times 100\% \tag{2}$$

where ΔH_m is the melting enthalpy of the blended membrane obtained from the DSC curve, ΔH_{PEO} denotes the value of

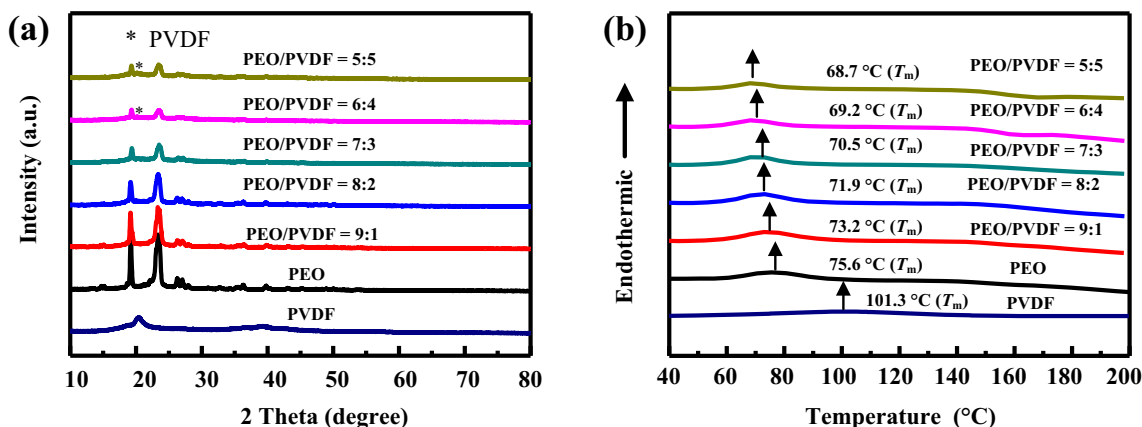


Fig. 2 a XRD patterns of the PEO/PVDF blend membrane at various compositions. b DSC curves of the PEO/PVDF blend membrane at various compositions

Table 1 DSC data for pure PEO and PEO/PVDF blends at various compositions

Code	Sample	Melting temp., T_m (°C)	Heat of fusion, ΔH_m (J/g)	Crystallinity, χ_c (%)
1	Pure PEO	75.6	154.3	72.2
2	PEO/PVDF = 9:1	73.2	127.2	66.1
3	PEO/PVDF = 8:2	71.9	108.6	63.5
4	PEO/PVDF = 7:3	70.5	91.3	61.0
5	PEO/PVDF = 6:4	69.2	82.9	64.6
6	PEO/PVDF = 5:5	68.7	74.8	70.0

213.7 J g⁻¹ for the perfect PEO crystal [23], and f_{PEO} is the PEO weight fraction of the blend membrane. The results in Table 1 show that the level of PEO/PVDF blend membrane crystallinity is decreased in comparison with that of the pure PEO, which could be attributed to the reciprocated suppression of the crystallization between PEO and PVDF. The blend attained the minimum crystallinity of 61.0% when the PEO/PVDF weight ratio is 7:3, which greatly reduced the PEO crystallinity and was a benefit for improving ionic conductivity.

The mechanical property of the PEO/PVDF blend membrane is evaluated to obtain safe CSEs. As shown in Fig. 3a, the pure PEO possesses the tensile strength of 4.8 MPa, whereas that of the PEO/PVDF blend is 7.0 MPa. Furthermore, the thermostability of the PEO/PVDF blend is investigated by TGA. As shown in Fig. 3b, the initial weight loss of the pure PEO occurs at 200 °C and is completed at 490 °C with a weight loss of 100 wt%. However, the remaining weight of the PEO/PVDF blend at 490 °C is approximately 30 wt%, which is close to the weight percent of the PVDF in the blend. In addition, the weight loss of 100 wt% for the PEO/

PVDF blend occurs at 540 °C. This result indicates that the prepared PEO/PVDF blend has superior thermostability.

Figure 4a shows the XRD patterns of the PEO/PVDF–LiTFSI and PEO/PVDF–LiTFSI–LLZO electrolytes and the as-prepared LLZO powder. A previous report [24] indicates that Li₇La₃Zr₂O₁₂ exists in two phases, namely, cubic and tetragonal. The former is more suitable for battery applications due to its giving superior lithium-ion conductivity (over 100 times higher than the latter). The result indicates that the as-prepared LLZO powders are a pure cubic phase (PDF: 45-0109), and the LLZO peak remains easy to observe after mixing with PEO/PVDF–LiTFSI. The SEM image in Fig. 4b (insert) shows that the size of LLZO particles is several tens nm, while the average size of LLZO powders (insert) is about 2.2 μm ($d_{50} = 2.155 \mu\text{m}$). The difference between the size of LLZO particles and the size of LLZO powders can be explained by aggregation of nanoparticles. For PEO/PVDF–LiTFSI–LLZO electrolyte (Fig. 4b, c), LLZO powders are homogeneously dispersed in PEO cell-type microstructures, which is beneficial to the enhancement of ionic mobility and mechanical strength [25–27].

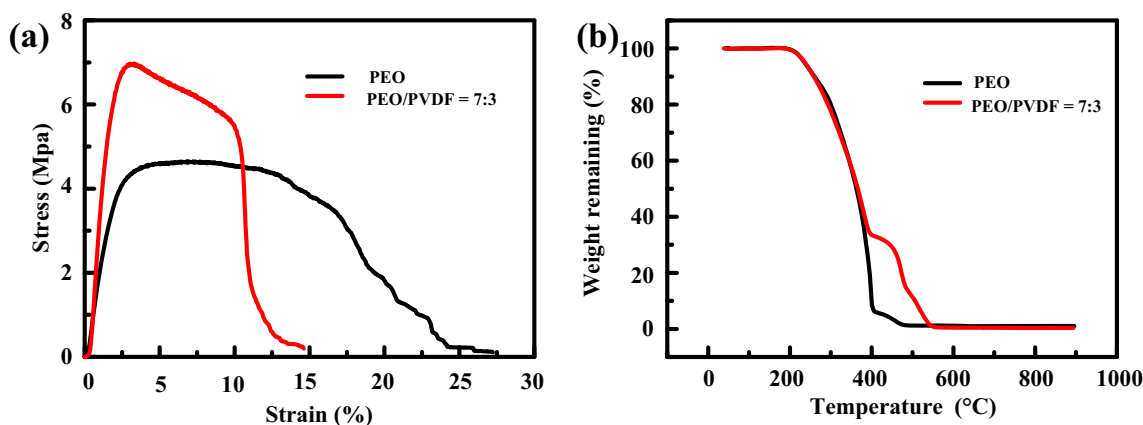
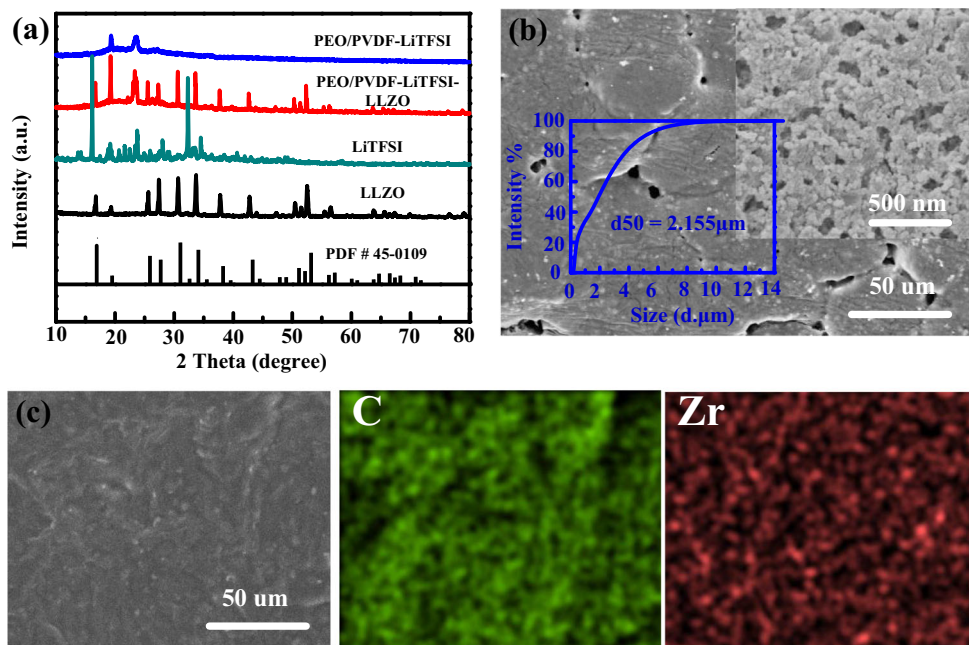
**Fig. 3** a Stress–strain curves for pure PEO and PEO/PVDF blend membrane. b TGA curves for pure PEO and PEO/PVDF blend membrane

Fig. 4 **a** XRD patterns of LLZO, LiTFSI, PEO/PVDF–LiTFSI–LLZO, and PEO/PVDF–LiTFSI. **b** SEM images of LLZO particles (insert), the size of LLZO powders (insert), and PEO/PVDF–LiTFSI–LLZO membrane. **c** EDS mapping images of C and Zr elements in the PEO/PVDF–LiTFSI–LLZO electrolyte



Generally, an electrolyte with a high ionic conductivity is a crucial parameter for the actual application of solid-state LIBs. The ionic conductivities of PEO/PVDF–LiTFSI–LLZO with different LLZO additive contents were investigated by AC impedance spectroscopy measurements. Figure 5a shows the impedance plots of the prepared PEO/PVDF–LiTFSI–LLZO with different LLZO additive contents. All plots appear with a semi-circle and an inclined straight tail. The total resistance of the CSEs can be estimated from the low-frequency intercept of the semi-circle on the Z' axis. Total resistance initially decreases and then increases with an increase of LLZO amount. The resistance reaches the minimum for the CSE doped with

10 wt% LLZO. The ionic conductivity calculated by substituting the resistance value into Eq. (1). As shown in Fig. 5b, the conductivities of all samples increase with the temperature. All the CSE curves show two linear regions (i.e., below and above 60 °C) because of different PEO crystallinities [8]. Furthermore, the conductivity of the CSE evidently initially increases and then decreases with the increase in LLZO content, and the CSE doped with 10 wt% LLZO exhibits the maximum ionic conductivity of $4.2 \times 10^{-5} \text{ S cm}^{-1}$ at 30 °C (Fig. 5c). The increase in total ion conductivity of CSEs can be explained by the additional pathway [28] that fast lithium-ion conducting LLZO provided, whereas the decrease may be due

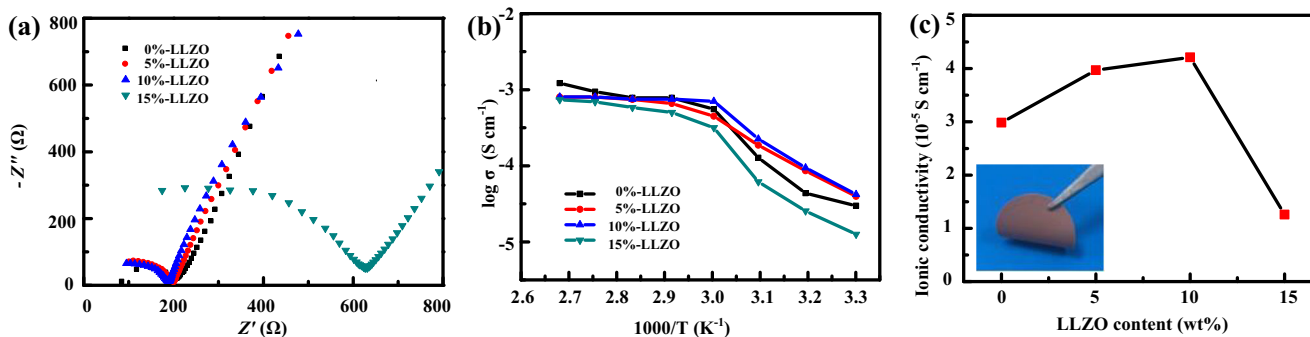


Fig. 5 **a** Impedance spectra of the CSEs with various LLZO contents measured at 30 °C. **b** Arrhenius plots of ionic conductivity for PEO/PVDF–LiTFSI–LLZO membrane with different LLZO additive

contents. **c** Ionic conductivity measured at 30 °C for PEO/PVDF–LiTFSI–LLZO membrane with different LLZO additive contents and the digital photograph of CSE doped with 10 wt% LLZO (insert)

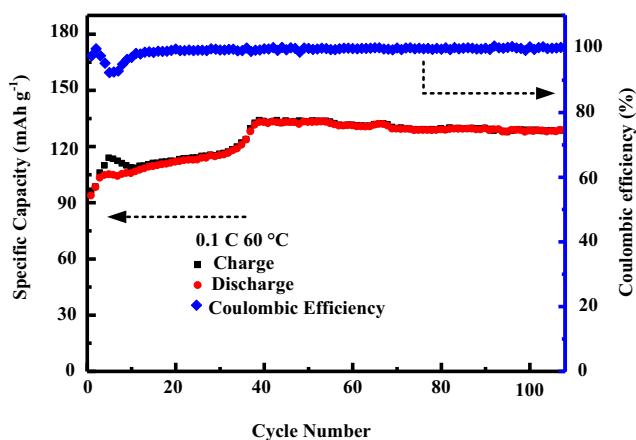


Fig. 6 Cycling performance and coulombic efficiency of all-solid-state battery $\text{LiFePO}_4/\text{CSE}|\text{Li}$ at 0.1 C for 100 cycles tested at 60 °C

to the aggregation of LLZO particles, which block the movement of PEO chains and increases the impedance between particles. In addition, the CSE doped with 10 wt% LLZO (in chocolate) exhibits good flexibility (insert of Fig. 5c).

Moreover, 2032-type coin cells with a lithium negative electrode and a LiFePO_4 positive electrode were fabricated (cycled between 2.5 and 3.9 V) to demonstrate the application of the PEO/PVDF–LiTFSI–10 wt% LLZO in all-solid-state LIBs. The cyclic performance of the all-solid-state lithium-ion batteries tested at 60 °C at 0.1 C is shown in Fig. 6. The first discharge-specific capacity of the all-solid-state battery is 93.6 mAh g^{-1} , which reaches 55.0% of the theoretical value of LiFePO_4 , and the discharge-specific capacity then increases with the cycles due to more electrolyte gradually penetrate into the inner part of the active materials [29, 30]. The cell delivers a maximum specific discharge capacity of 133.0 mAh g^{-1} after four 10 cycles. The discharge capacities of the cell

remain at 128.3 mAh g^{-1} after 100 cycles, which suggests that 96.5% of their maximum capacities are retained. Furthermore, the coulombic efficiency is close to 100% after two 10 cycles.

In all-solid-state LIBs, the inhibiting growth of lithium dendrite is also an important criterion in electrolyte assessment. The performance was investigated by galvanostatic cycling experiments with $\text{Li}|\text{Li}$ symmetric cell structure at 60 °C, in which lithium was stripped from one electrode and plated on another by charging/discharging for 0.5 h. As shown in Fig. 7a, both cells ($\text{Li}|\text{PEO}/\text{PVDF}-\text{LiTFSI}|\text{Li}$ cell and $\text{Li}|\text{PEO}/\text{PVDF}-\text{LiTFSI}-\text{LLZO}|\text{Li}$ cell) can cycle stably more than 250 h at a current density of 0.05 mA cm^{-2} . Moreover, both cells have almost the same small voltage value ($< 5 \text{ mV}$). To better compare the property of suppressing lithium dendrite growth, both cells also cycled at high current density (0.2 mA cm^{-2}). As shown in Fig. 7b, the symmetric $\text{Li}|\text{PEO}/\text{PVDF}-\text{LiTFSI}|\text{Li}$ cell could only be steadily cycled only for $\sim 200 \text{ h}$, and a short-circuit phenomenon occurred after 200 h because of uneven lithium electrodeposition [31, 32] that usually led to the lithium dendrite formation. Nevertheless, at the same current density, the symmetric $\text{Li}|\text{PEO}/\text{PVDF}-\text{LiTFSI}-\text{LLZO}|\text{Li}$ cell shows considerably more cycling stability and superior voltage profiles. These results indicate that PEO/PVDF–LiTFSI–LLZO electrolyte membrane has a superior property of suppressing lithium dendrite growth during a long-term cycle.

Figures 8a, b compare the fire resistance properties of the traditional commercially used Celgard separator and the CSE electrolyte prepared in this study. The Celgard separator decomposes immediately as it comes close to the flame, which indicates poor inflaming retardation (Fig. 8a). In comparison, the CSE electrolyte developed in this study can retain its shape for more than 15 s (Fig. 8b). This high inflaming retardation is

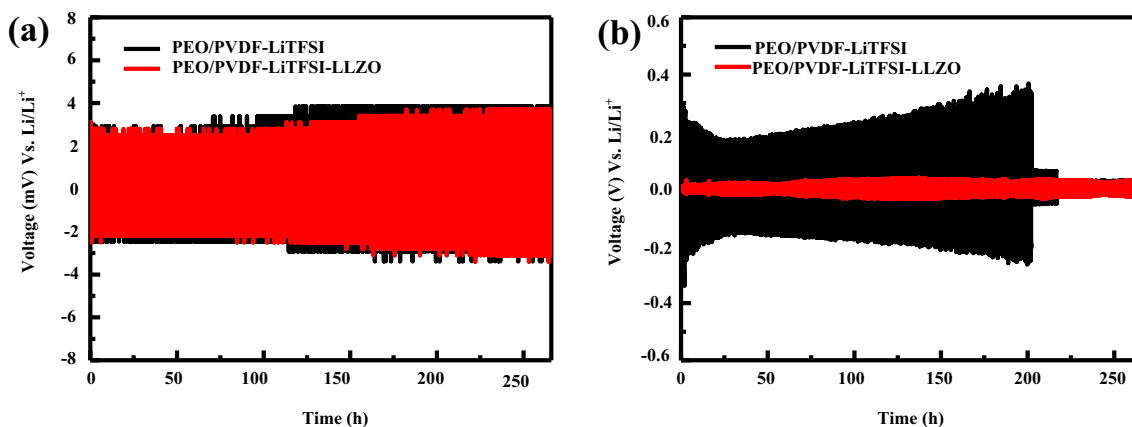
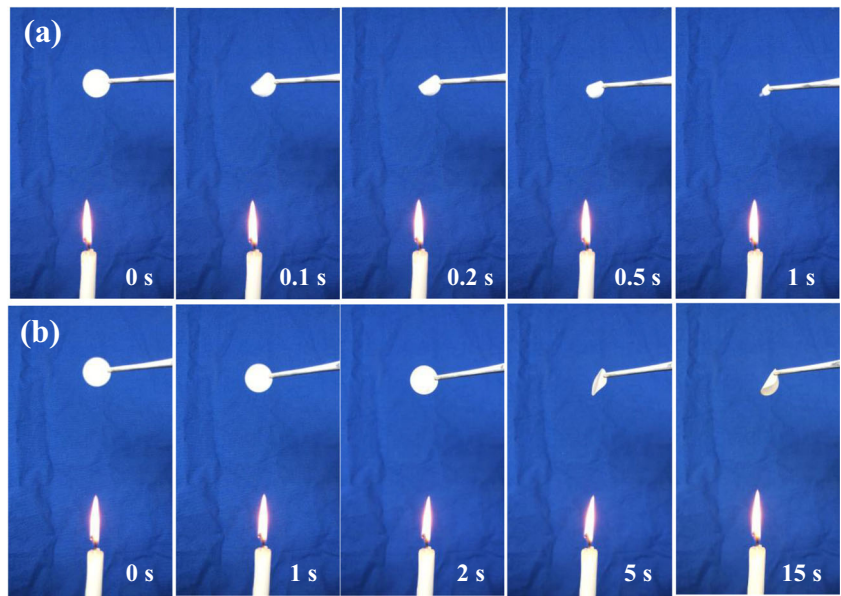


Fig. 7 Galvanostatic cycling curves of the symmetric $\text{Li}|\text{CSE}|\text{Li}$ cell at current density of **a** 0.05 mA cm^{-2} and **b** 0.2 mA cm^{-2}

Fig. 8 Flammability test of **a** Celgard and **b** PEO/PVDF–LiTFSI–LLZO electrolyte membrane



due to the good thermostability of the PEO/PVDF matrix and the addition of LLZO. These results imply that the electrolyte in this study is a good component for the safety problems in LIBs.

Conclusions

A new composite solid electrolyte membrane consisting of PEO/PVDF matrix, LiTFSI, and LLZO powders was prepared by blending technique combined with adding ceramic solid electrolytes. The addition of 30 wt% of PVDF into the PEO yielded a low melting point and crystallinity PEO/PVDF matrix, which is beneficial for the improvement of ionic conductivity. Meanwhile, the PEO/PVDF matrix showed superior mechanical strength and thermostability in comparison with the pure PEO matrix. The addition of LLZO powders further improved the ionic conductivity. Approximately one and a half times of enhancement in ionic conductivity was achieved by adding 10 wt% LLZO. All-solid-state LIBs using this CSE, lithium metal anode, and LiFePO_4 cathode showed a remarkable cyclic stability and excellent coulombic efficiency (close to 100%) and retained 96.5% of the maximum capacity after 100 cycles. Furthermore, the CSE could effectively inhibit lithium dendrite growth due to the lithium plating/stripping determination of the Li|Li symmetric cell using the electrolyte cycled for more than 300 h at 0.2 mA cm^{-2} at $60 \text{ }^\circ\text{C}$. The results indicated that the CSE in this study is a hopeful candidate for next-generation all-solid-state LIBs.

Acknowledgements This work was supported by the National Nature Science Foundation of China (NSFC no. 51672130, 51572123), the Key Research and Development Program of Jiangsu Province (grant no. BE2018008-2), the Research Fund of State Key Laboratory of Mechanics and Control of Mechanical Structures (Nanjing University of Aeronautics and astronautics) (grant no. MCMS-0518K01), the special fund of 333 high-level talents training project in Jiangsu province (BRA2017424), and A Project Funded by the Priority Academic Program Development of Jiangsu Higher Education Institutions (PAPD).

References

- Kim JG, Son B, Mukherjee S, Schuppert N, Bates A, Kwon O, Choi MJ, Chung HY, Park S (2015) A review of lithium and non-lithium based solid state batteries. *J Power Sources* 282:299–322
- Youcef HB, Garcia-Calvo O, Lago N, Devaraj S, Armand M (2016) Cross-linked solid polymer electrolyte for all-solid-state rechargeable lithium batteries. *Electrochim Acta* 220:587–594
- Li Y, Fan C, Zhang J, Wu X (2018) A promising PMHS/PEO blend polymer electrolyte for all-solid-state lithium ion batteries. *Dalton Trans* 47:14932–14937
- Polu AR, Rhee HW (2015) Nanocomposite solid polymer electrolytes based on poly (ethylene oxide)/POSS-PEG ($n = 13.3$) hybrid nanoparticles for lithium ion batteries. *J Ind Eng Chem* 31:323–329
- Sasithorn K, Pumchusak J (2015) Effects of nano alumina and plasticizers on morphology ionic conductivity, thermal and mechanical properties of PEO- LiCF_3SO_3 solid polymer electrolyte. *Electrochim Acta* 161:171–176
- Zhang W, Nie J, Li F, Wang Z, Sun C (2018) A durable and safe solid-state lithium battery with a hybrid electrolyte membrane. *Nano Energy* 45:413–419
- Choi KH, Cho SJ, Kim SH, Kwon YH, Kim JY, Lee SY (2014) Thin, deformable, and safety-reinforced plastic crystal polymer

- electrolytes for high-performance flexible lithium-ion batteries. *Adv Funct Mater* 24:44–52
8. Xue Z, He D, Xie X (2015) Poly(ethylene oxide)-based electrolytes for lithium-ion batteries. *J Mater Chem A* 3:19218–19253
 9. Zhang J, Huang X, Wei H, Fu J, Huang Y, Tang X (2010) Novel PEO-based solid composite polymer electrolytes with inorganic-organic hybrid polyphosphazene microspheres as fillers. *J Appl Electrochem* 40:1475–1481
 10. Sun C, Liu J, Gong Y, Wilkinson DP, Zhang J (2017) Recent advances in all-solid-state rechargeable lithium batteries. *Nano Energy* 33:363–386
 11. Wang Y, Pan Y, Wang L, Pang M, Chen L (2005) Conductivity studies of plasticized PEO-Lithium chlorate-FIC filler composite polymer electrolytes. *Mater Lett* 59:3021–3026
 12. Lee L, Park SJ, Kim S (2013) Effect of nano-sized barium titanate addition on PEO/PVDF blend-based composite polymer electrolytes. *Solid State Ionics* 234:19–24
 13. Tao C, Gao M, Yin B, Li B, Huang Y, Xu G, Bao J (2017) A promising TPU/PEO blend polymer electrolyte for all-solid-state lithium ion batteries. *Electrochim Acta* 257:31–39
 14. Fan L, Dang Z, Nan C, Li M (2002) Thermal, electrical and mechanical properties of plasticized polymer electrolytes based on PEO/P(VDF-HFP) blends. *Electrochim Acta* 48:205–209
 15. Zhao Y, Wu C, Peng G, Chen X, Yao X, Bai Y, Wu F, Chen S, Xu X (2016) A new solid polymer electrolyte incorporating $\text{Li}_{10}\text{GeP}_2\text{S}_{12}$ into a polyethylene oxide matrix for all-solid-state lithium batteries. *J Power Sources* 301:47–53
 16. Jung YC, Lee SM, Choi JH, Jang SS, Kim DW (2015) All solid-state lithium batteries assembled with hybrid solid electrolytes. *J Electrochem Soc* 162:A704–A710
 17. Li Y, Yang T, Wu W, Cao Z, He W, Gao Y, Liu J, Li G (2018) Effect of Al-Mo codoping on the structure and ionic conductivity of sol-gel derived $\text{Li}_7\text{La}_3\text{Zr}_2\text{O}_{12}$ ceramics. *Ionics* 24:3305–3315
 18. Wang M, Sakamoto J (2018) Dramatic reduction in the densification temperature of garnet-type solid electrolytes. *Ionics* 24:1861–1868
 19. Wu J, Chen E, Yu Y, Liu L, Wu Y, Pang W, Peterson VK, Gu X (2017) Gallium-doped $\text{Li}_7\text{La}_3\text{Zr}_2\text{O}_{12}$ garnet-type electrolytes with high lithium-ion conductivity. *ACS Appl Mater Interfaces* 9:1542–1552
 20. Wu J, Pang W, Peterson V, Wei L, Guo X (2017) Garnet-type fast Li-ion conductors with high ionic conductivities for all-solid-state batteries. *ACS Appl Mater Interfaces* 9:12461–12468
 21. Chen F, Yang D, Zha W, Zhu B, Zhang Y, Li J, Gu Y, Shen Q, Zhang L, Sadoway DR (2017) Solid polymer electrolytes incorporating cubic $\text{Li}_7\text{La}_3\text{Zr}_2\text{O}_{12}$ for all-solid-state lithium rechargeable batteries. *Electrochim Acta* 258:1106–1114
 22. Saikia D, Chen-Yang YW, Chen YT, Li YK, Lin SI (2008) Investigation of ionic conductivity of composite gel polymer electrolyte membranes based on P(VDF-HFP), LiClO_4 and silica aerogel for lithium ion battery. *Desalination* 234:24–32
 23. Jinisha B, Anilkumar KM, Manoj M, Pradeep VS, Jayalekshmi S (2017) Development of a novel type of solid polymer electrolyte for solid state lithium battery applications based on lithium enriched poly(ethylene oxide) (PEO)/poly(vinyl pyrrolidone) (PVP) blend polymer. *Electrochim Acta* 235:210–222
 24. Geiger CA, Alekseev E, Lazic B, Fisch M, Armbruster T, Langner R, Fechtelkord M, Kim N, Pettke T, Weppner W (2011) Crystal chemistry and stability of " $\text{Li}_7\text{La}_3\text{Zr}_2\text{O}_{12}$ " garnet: a fast lithium-ion conductor. *Inorg Chem* 50:1089–1097
 25. He Z, Chen L, Zhang B, Liu Y, Fan L (2018) Flexible poly(ethylene carbonate)/garnet composite solid electrolyte reinforced by poly(vinylidene fluoride-hexafluoropropylene) for lithium metal batteries. *J Power Sources* 392:232–238
 26. Zhang X, Xu B, Lin Y, Shen Y, Li L, Nan C (2018) Effects of $\text{Li}_{6.75}\text{La}_3\text{Zr}_{1.75}\text{Ta}_{0.25}\text{O}_{12}$ on chemical and electrochemical properties of polyacrylonitrile-based solid electrolytes. *Solid State Ionics* 327:32–38
 27. Tao X, Liu Y, Liu W, Zhou G, Zhao J, Lin D, Zu C, Sheng O, Zhang W, Lee H, Cui Y (2017) Solid-state lithium-sulfur batteries operated at 37 °C with composites of nanostructured $\text{Li}_7\text{La}_3\text{Zr}_2\text{O}_{12}$ /carbon foam and polymer. *Nano Lett* 17:2967–2972
 28. Cheng SHS, He KQ, Liu Y, Zha JW, Kamruzzaman M, Ma RLW, Dang ZM, Li RKY, Chung CY (2017) Electrochemical performance of all-solid-state lithium batteries using inorganic lithium garnets particulate reinforced PEO/ LiClO_4 electrolyte. *Electrochim Acta* 253:430–438
 29. Wu F, Xiong S, Qian Y, Yu S (2015) Hydrothermal synthesis of unique hollow hexagonal prismatic pencils of $\text{Co}_3\text{V}_2\text{O}_8 \cdot n\text{H}_2\text{O}$: a new anode material for lithium-ion batteries. *Angew Chem Int Edit* 54:10787–10791
 30. Zhao S, Li H, Jian Z, Xing Y, Zhang S (2018) Self-assembled hierarchical porous NiMn_2O_4 microspheres as high performance Li-ion battery anodes. *Rsc Adv* 8:41749–41755
 31. Choudhury S, Mangal R, Agrawal A, Archer LA (2015) A highly reversible room-temperature lithium metal battery based on crosslinked hairy nanoparticles. *Nat Commun* 6:10101
 32. Pan Q, Smith DM, Qi H, Wang S, Li CY (2015) Hybrid electrolytes with controlled network structures for lithium metal batteries. *Adv Mater* 27:5595–6001

Publisher's note Springer Nature remains neutral with regard to jurisdictional claims in published maps and institutional affiliations.